

# Absorption Saturation is Tailorable in the Strong Light-Matter Coupling Regime

Raffaele Colombelli\* and Mathieu Jeannin†

Centre de Nanosciences et de Nanotechnologies (C2N),  
CNRS UMR 9001, Université Paris-Saclay, 91120 Palaiseau, France

(Dated: January 1, 2021)

It is well known that optical absorption saturation of intersubband transitions in doped semiconductor quantum wells is independent of the introduced doping in the absence of a cavity. When inserting the system in a resonator, we show that this remains valid only in the weak light-matter coupling regime. In the strong light-matter coupling regime instead, we demonstrate that absorption saturation is no more doping independent and it is instead tailorable. Based on this unified formalism for saturation in weak and strong coupling, we provide designs for semiconductor saturable absorption (SESAM) mirrors and bistable systems operating in the mid-infrared range of the electromagnetic spectrum and with extremely low saturation intensities. Countering intuition, we show that the most suitable region to exploit low saturation intensities is not the ultra-strong coupling regime, but is instead at the onset of strong light-matter coupling.

Saturation of the light-matter interaction (optical absorption saturation) is a general feature of material systems, be they atoms or semiconductors: provided that a sufficiently high optical power is employed, the absorption decreases as the material departs more and more from its ground state [1]. In particular in semiconductors, the possibility of judiciously controlling, or engineering, saturation phenomena is of great importance for applications as well as basic physics.

A seminal example is the development of the semiconductor saturable absorption mirror (SESAM) [2], based on interband transitions in semiconductor quantum wells (QW), that revolutionized the field of ultra-fast lasers in the visible/near-IR spectral range. Ultra-fast lasers based on SESAMs now find applications in several domains, and research is starting to exploit them towards the exploration of subtle quantum phenomena [3].

A possible consequence of saturable absorption - under specific conditions - is optical bistability [1], that manifests itself as an hysteresis cycle when plotting the input-vs-output characteristic of the system. Besides its interest as a fundamental phenomenon that stems from a non-parametric non-linear process, it has been proposed in the past as a strategy for optical information processing. Beautiful proposals [4] and demonstrations [5] exist in the domain of excitonic polaritons.

A saturable absorber exhibits an absorption coefficient that depends on the incident intensity  $I$  as follows:

$$\alpha = \frac{\alpha_0}{1 + I/I_{sat}} \quad (1)$$

$\alpha_0$  is the absorption at low incident power, and  $I_{sat}$  is the saturation intensity. At  $I_{sat}$ , the absorption is 50% of the low-intensity value. The saturation intensity in general depends on the precise characteristics of the system: lifetimes, oscillator strengths/dipoles, operating frequency.... The only available way to engineer it is to act

on the system lifetimes. However, the saturation intensity levels for systems based on *interband* transitions in semiconductors are favorable for a vast range of applications in the visible/near-IR spectral ranges.

The case is different for *intersubband transitions* (ISBT) in semiconductor QWs, that are the backbone of semiconductor-based mid-IR optoelectronics (quantum cascade lasers and QW infrared detectors) [6–8]. Considering a Brewster angle incidence (Fig. 1(a)) or a multipass configuration, the classical theory provides the following value for the saturation intensity in the absence of a cavity/resonator [9][10]:

$$I_{sat}^{no-cav} = \frac{\hbar^2 \varepsilon_0 c n_{opt}}{2e^2 \tau_{12} T_2 |\langle 1|z|2\rangle|^2} = \frac{\varepsilon_0 c n_{opt}}{2\tau_{12} T_2 |D_{12}/\hbar|^2} \quad (2)$$

where  $n_{opt}$  is an average index of refraction of the active region,  $\tau_{12}$  is upper state lifetime,  $T_2$  is the dephasing time,  $|\langle 1|ez|2\rangle| = D_{12}$  is the electric dipole matrix element. In the mid-IR ( $\lambda = 10 \mu\text{m}$ ) we obtain  $I_{sat}$  values of the order of 1 MW/cm<sup>2</sup>, as confirmed by a vast body of literature [11–13].

This very high value explains why saturable absorbers, SESAM mirrors, bistable systems are missing from the current toolbox of mid-IR opto-electronic devices: they could be used only with extremely high power laser sources, and are in particular incompatible with the typical output power levels of quantum cascade lasers (QCL) [14].

In this letter, we demonstrate that the nature of absorption saturation for an ISB system is radically modified in the strong light-matter coupling regime. We develop a unified analytical formalism for absorption saturation in weak (WCR) and strong (SCR) regime. It permits to show that it is possible to engineer, and therefore to reduce  $I_{sat}$ , with a vast number of opportunities opening up as a consequence, such as the emergence of optical bistability [15]. We provide a set of simple analytical formulas that permit to quickly assess the saturation power levels for a given ISB system in weak or strong coupling.

Eq. 2 reveals that  $I_{sat}^{no-cav}$  does not depend on the doping level in the QW (Fig. 1, bottom left panel). One

\* E-mail: raffaele.colombelli@u-psud.fr

† E-mail: mathieu.jeannin@u-psud.fr

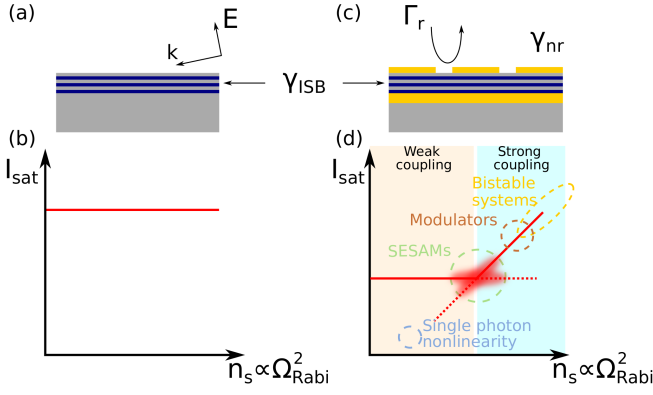


Figure 1. (a) Typical geometry for the derivation of  $I_{sat}^{no-cav}$  [9] with no resonator. (b) In this case,  $I_{sat}^{no-cav}$  is independent on the sheet doping per QW  $n_s$ . (c) Sketch of the system in the presence of a metal-insulator-metal (MIM) grating. (d) If the system operates in weak coupling (yellow region), the value of  $I_{sat}$  can be affected by the cavity, but still does not depend on  $n_s$ . However, as soon as the system enters the strong coupling regime (SCR), the saturation intensity increases linearly with the doping. Dotted lines represent extrapolations that would be attainable by changing the system parameters. In an ISB system engineered to operate in the SCR down to very low doping levels,  $I_{sat}$  can be almost arbitrarily reduced.

might think that this stems from the absence of a resonator. It is in fact a general feature when the system operates in the weak-coupling regime (WCR) between light and matter: the absolute value of  $I_{sat}$  can be engineered using a cavity, but its independence of the introduced doping density persists.

Let's model the saturation with a simple rate equation approach. The steady-state expression of the electronic population for the second subband of a system of doped QWs with surface charge density per QW  $n_s$  is:

$$n_2 = \frac{I}{\hbar\omega} \tau_{12} \mathcal{A}^{qw}(\Delta n, \omega) = \frac{I}{N_{qw} \hbar\omega} \tau_{12} \mathcal{A}^{ISB}(\Delta n, \omega) \quad (3)$$

where  $n_2$  is the charge surface density in the excited subband,  $I$  is the incident intensity per unit surface,  $\tau_{12}$  is the upper state lifetime,  $N_{qw}$  is the number of QWs,  $\mathcal{A}^{qw}(\Delta n, \omega)$  is the absorption per QW,  $\mathcal{A}^{ISB}(\Delta n, \omega)$  is the total absorption of the ISB system, and  $\Delta n = n_1 - n_2$  is the population difference.

The saturation condition is defined as:

$$n_2 = \frac{n_s}{4} \iff \Delta n = \frac{n_s}{2} \quad (4)$$

The saturation intensity is therefore obtained from the following equation:

$$\frac{n_s}{4} = \frac{I_{sat}}{N_{qw} \hbar\omega} \tau_{12} \mathcal{A}^{ISB}\left(\frac{n_s}{2}, \omega\right) \quad (5)$$

As far as the absorption from the ISB system can be written as a *linear* term in the doping density  $n_s$ ,  $I_{sat}$  is

doping independent. This is usually the case, as the absorption links to the imaginary part of the permittivity, that is a dielectric tensor whose growth-direction component  $\varepsilon_{zz}$  - the one that couples to the ISB dipole - can be typically cast in the following form [16]:

$$\frac{1}{\varepsilon_{zz}(\omega)} = \frac{1}{\varepsilon_{avg}} \left( 1 + \frac{\omega_p^2}{\omega^2 - \omega_{12}^2 + i\gamma\omega} \right) \quad (6)$$

$\omega_{12}$ ,  $\gamma$  and  $\omega_p$  are the resonant frequency, the homogeneous linewidth, and the plasma frequency, respectively. The plasma frequency being defined as:

$$\omega_p^2 = \frac{n_s e^2}{\varepsilon_0 \varepsilon_{avg} m^* L_{qw}} \quad (7)$$

(with  $m^*$  the QW effective mass, and  $L_{qw}$  its width), the linear dependence on  $n_s$  is respected and  $I_{sat}$  is doping independent, as schematized in the *weak coupling* region of Fig. 1(d) (yellow region).[17]

The situation radically changes if the system enters the strong coupling regime (SCR). The crucial difference is that  $\mathcal{A}^{ISB}(n_s, \omega)$  is no more a linear function of the doping, but is instead independent of  $n_s$ , as sketched in Fig. 2(a). This is an established fact (see for instance Ref. [18], Supporting Info), albeit of little resonance, that can be intuitively understood as follows: in the WCR, increasing  $n_s$  leads to an increase of  $\Im(\varepsilon_{zz}(\omega))$  and therefore of the absorption. In the SCR instead, all increase in  $n_s$  translates in an increase of  $\Omega_{Rabi} \propto \omega_p$ , with no further augmentation of the system absorption[19].

From Eq. 5 it is straightforward to infer a saturation intensity that increases linearly with  $n_s$  in strong coupling. The intuitive picture is resumed in Fig. 1(d). It reveals that - as long as the system operates in SCR,  $I_{sat}$  can be engineered, and each regime suits a different application. Ultra-fast modulators relying on SCR, as in Ref. [20], suit the strong/ultra-strong coupling regime, as it is important that they do not easily saturate. SESAM mirrors best fit the onset of SCR, as low  $I_{sat}$  can be achieved, retaining at the same time a high reflectivity in the saturated state. A final interesting perspective is the regime of ultra-low power nonlinearities in the mid-IR. While this requires very low loss resonators and is thus beyond the scope of this paper, we speculate that mid-IR on-chip III-V photonics is a suitable platform [21].

We will now employ analytical simulations (temporal coupled mode theory, TCMT) to gain a quantitative understanding of this phenomenon. In this framework, the cavity mode and the ISB system are modelled as oscillators with characteristic parameters ( $\omega_i, \gamma_i, \Gamma_i$ ) representing respectively their natural oscillation frequency, non-radiative, and radiative dampings [22] In the case of the ISB system, the direct radiative coupling of the ISB transition to free-space radiation is very weak, [23] so we can neglect the corresponding radiative damping [18]. The response of the coupled system to an external excitation

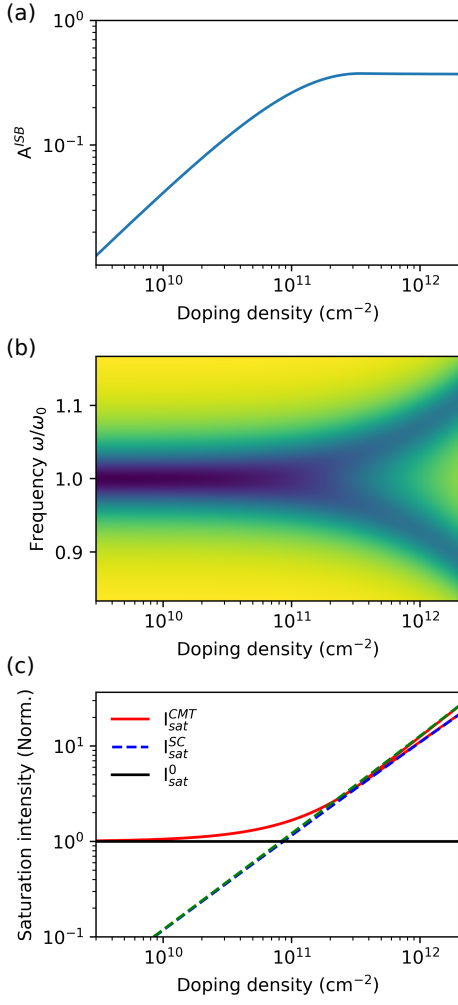


Figure 2. (a) Intersubband absorption  $\mathcal{A}^{ISB}(n_s, \omega)$  as a function of  $\Omega_{Rabi}^2$  or - equivalently - the doping density  $n_s$ . In weak coupling, the absorbance of the ISB system is a linear function of  $n_s$ . As soon as the system transitions to the SCR,  $\mathcal{A}^{ISB}(n_s, \omega)$  does not increase any more. (b) Reflectivity of the system as a function of  $n_s$  for a weak probe intensity. The onset of the polaritonic states correspond to the *locking* of  $\mathcal{A}^{ISB}(n_s, \omega)$  to its maximum value. (c) Saturation intensity normalized to the low-doping value ( $I_{sat}/I_{sat}^{n_s \rightarrow 0}$ ) as a function of  $n_s$ . The black solid line is the asymptotic saturation intensity in the WCR  $I_{sat}^0$ , and the two dashed lines are the asymptotic saturation intensity  $I_{sat}^{SC}$  in the SCR corresponding to the lower (blue) and upper (green) polaritons. The red solid line corresponds to the analytical solution  $I_{sat}^{\pm, CMT}$ .

is then given by the following set of equations:

$$\frac{da_{isb}}{dt} = (i\omega_{isb} - \gamma_{isb})a_{isb} + i\Omega_{Rabi}a_c \quad (8)$$

$$\frac{da_c}{dt} = (i\omega_c - \gamma_{nr} - \Gamma_r)a_c + i\Omega_{Rabi}a_{isb} + \sqrt{2\Gamma_r}s^+ \quad (9)$$

$$s^- = -s^+ + \sqrt{2\Gamma_r}a_c \quad (10)$$

$$n_2 = 2\tau_{12}\gamma_{isb} \frac{|a_{isb}|^2}{N_{qw}\hbar\omega} \quad (11)$$

where  $a_i$  is the amplitude of oscillator  $i$  referencing either the ISB system ( $i = isb$ ) or the cavity ( $i = c$ ),  $\gamma_{isb}$  and  $\gamma_{nr}$  correspond respectively to the non-radiative decay rate of the ISB transition and of the cavity,  $\Gamma_r$  is the cavity radiative decay rate,  $s^+$  is the amplitude of the incoming driving field, and  $s^-$  the amplitude of the reflected field.

The coupling rate between the two oscillators is simply the vacuum Rabi frequency, which depends on the excited state population:

$$\Omega_{Rabi}^2 = f_w \frac{\Delta n e^2}{4\epsilon\epsilon_0 m^* L_{qw}} = a \Delta n \quad (12)$$

where  $f_w$  is the filling fraction of the QWs material in the active region. Equations (11) and (12) ensure the self-consistency of the set of CMT equations. Solving this system in the harmonic regime, where  $s^+ = e^{i\omega t}$ , we derive both the reflectivity of the coupled system  $R = \left| \frac{s^-}{s^+} \right|^2$  (see Suppl. Mat.) and the absorption of the sole ISB system:

$$\begin{aligned} \mathcal{A}^{ISB} &= 2\gamma_{isb} \left| \frac{a_{isb}}{s^+} \right|^2 \\ &= \frac{4\gamma_{isb}\Gamma_r\Omega_{Rabi}^2}{[\gamma_{isb}(\gamma_{nr} + \Gamma_r) - ((\omega - \omega_0)^2 - \Omega_{Rabi}^2)]^2 + (\gamma_{isb} + \gamma_{nr} + \Gamma_r)^2(\omega - \omega_0)^2} \end{aligned} \quad (13)$$

where we further assumed without loss of generality that the cavity and ISB system are resonant ( $\omega_{isb} = \omega_c = \omega_0$ ).

Using the above set of equations, we study the response of the cavity-coupled ISB system as a function of the doping density  $n_s$  for a weak probing beam. The maximum ISB absorption following eq. (13) is shown in Fig. 2(a). As discussed previously, two regimes appear clearly: for low carrier density the absorption increases linearly with the doping density, while for large dopings the maximum ISB absorption flattens and becomes independent of the doping.

These two regimes also appear as a clear change in the spectral response of the system as shown in the reflectivity map in Fig. 2(b): the transition from the weak to the strong coupling regime is characterized by an energy splitting of the two (degenerate) resonances. The expression of the ISB absorption (13) can be simplified in the two limiting cases of either very low doping (WCR) or large doping (SCR).

Plugging these asymptotic values of  $\mathcal{A}^{ISB}$  (Suppl. Mat.) into eq. (5) leads to the following practical analytical expressions for the saturation intensity:

$$I_{sat}^0 = \frac{\hbar\omega_0\epsilon\epsilon_0 m^* L_{qw} N_{qw} \gamma_{isb}(\gamma_{nr} + \Gamma_r)^2}{2\tau_{12} f_w e^2 \Gamma_r} \quad (14)$$

$$I_{sat}^{SC} = \frac{n_s \hbar\omega_{\pm} N_{qw} (\gamma_{isb} + \gamma_{nr} + \Gamma_r)^2}{16\tau_{12} \gamma_{isb} \Gamma_r} \quad (15)$$

where  $\omega_{\pm}$  represents the polariton frequencies.  $I_{sat}^0$  represents the limit of low doping, where the system

operates in the weak coupling regime, and is evidently independent of the doping density  $n_s$ .

Conversely,  $I_{sat}^{SC}$  corresponds to a system operating in the strong coupling regime, where the saturation intensity increases linearly with  $n_s$  and with  $N_{qw}$ . These two asymptotic expressions confirm the discussion above based on qualitative arguments.

It is worth re-arranging the weak coupling limit expression (14) to highlight the key parameters governing the reduction in  $I_{sat}$ .

$$I_{sat}^0 = f_{osc} \frac{\pi L_{AR}}{(\lambda/n_{opt})} \frac{Q_r}{2 \cdot Q_{tot}^2} \cdot I_{sat}^{no-cav} \quad (16)$$

where  $f_{osc}$  is the ISB oscillator strength [6],  $L_{AR}$  is the total thickness of the active region, and  $Q_r$  and  $Q_{tot}$  are the cavity radiative and total Q-factor, respectively. Eq. 16 explicitly links the lowest saturation intensity one can achieve in a cavity-coupled system ( $I_{sat}^0$ ) to the cavity-free one. The reduction factor deserves a more careful inspection. Setting aside the oscillator strength  $f_{osc}$ , the reduction in saturation intensity is directly linked to the cavity thickness and quality factors.

The two asymptotic regimes are shown in Fig. 2(c) ( $I_{sat}^0$  in black solid line and  $I_{sat}^{SC}$  in dashed lines). The strong-coupling limit is twofold since the upper/lower polariton frequencies split apart upon increasing the doping. The exact analytical solution is obtained by substituting eq. (13) in eq. (5) (red solid line), demonstrating the system's behaviour around the crossing point, and confirming the intuitive picture of Fig. 1(d). The set of equations 14 – 16 constitute a practical analytical toolbox to gauge and/or engineer the absorption saturation in any ISB system.

We rely on the ideas developed above to devise a semiconductor-based saturable system operating with ultra-low  $I_{sat}$  at mid-IR wavelengths ( $\omega_0 = 30$  THz,  $\lambda = 10 \mu\text{m}$ ) and based on ISB transitions in QWs. A superficial inspection of Fig. 2(c) suggests that the lower the doping, the better. However, saturation would be almost undetectable in a MIM cavity operating in the WCR, since the losses are dominated by the cavity, and the saturated/non-saturated reflectivity spectra would be almost identical. It is therefore necessary to operate in the SCR, where saturation would lead to clear spectral changes. Equation 15 clarifies that the system will have to operate at the onset of SC, embed the lowest possible number of QWs, and the lowest possible sheet doping per QW allowing operation in the SCR. Let's consider a system composed of 4 periods of GaAs/Al<sub>0.33</sub>Ga<sub>0.67</sub>As (8.3 nm/14 nm), with the barriers  $\delta$ -doped to  $n_s = 3 \cdot 10^{11} \text{ cm}^{-2}$ , embedded in metal-metal patch-cavity resonators (see Fig. 3(a)) [24]. Patch resonators have been successfully used for mid-IR applications (polaritons, second-harmonic generation, detectors) [25–27]. The total structure thickness (once in a MIM configuration) is  $\approx 140$  nm, and the overlap factor is  $f_w \approx 0.24$ .

We first numerically calculate the system reflectivity when in strong coupling with a patch cavity mode at low

incident power. Figure 3(b) (blue curve) is obtained from finite elements method (FEM) simulations: the UP and LP modes are clearly visible. The black curve shows instead the saturated system ( $I > I_{sat}$ ).

The regions highlighted in light blue correspond to an absorption that *decreases* with incident power: they suit the development of SESAM mirrors. The region highlighted in orange correspond to an absorption that *increases* with incident power: under specific conditions, a bistable system could be implemented here.

Let's now employ the TCMT to estimate  $I_{sat}$  for this sample/device: the results are reported in Fig. 3(c). We fix the non-radiative damping rate of the ISB system with typical intersubband absorption Q factors, so that  $\gamma_{isb} = 0.05\omega_c$ . The radiative and non-radiative damping rates of the cavity are determined from finite element method simulations, respectively  $\gamma_{nr} = 0.02\omega_c$  and  $\Gamma_r = 0.02\omega_c$  [28]. From the equations above, we obtain a WCR limit value of  $I_{sat}^0 = 3.45 \text{ kW/cm}^2$ . Considering the previously chosen doping level of  $3 \cdot 10^{11} \text{ cm}^{-2}$  per QW, we obtain  $I_{sat}^{SC} = 14.7 \text{ kW/cm}^2$ , with a Rabi frequency  $\Omega_{Rabi} \approx 3 \text{ THz}$ . Note that the saturation intensity of the same active region in absence of a cavity following eq. (2) is of the order of  $I_{sat}^{no-cav} = 1.1 \text{ MW.cm}^{-2}$ . Our approach thus allows at least an eighty-fold reduction of the saturation intensity.

This would already be a record-low value for mid-IR absorption saturation in an ISB system. However, it is actually an upper limit as we have to take into account the enhancement in absorption cross-section of the system. This is a general feature: as the effective capture area of a sub-wavelength resonant dipole is approximately  $3\lambda^2/8\pi$  [29], an array of sub-wavelength resonators (patch cavities in this case) can effectively collect photons over an area greater than its physical area. The topic is discussed in several references (see for instance non-linear meta-surfaces [26], optical antennas [30], detectors [31]) and while we will not detail it here we can provide an estimate. From a numerical simulation of the system schematized in Fig. 3(a) we find that  $s = 1.2 \mu\text{m}$  and  $p = 2.2 \mu\text{m}$  is an optimal configuration. In such geometry, the active surface covers 30% of the unit cell surface. This leads to an enhancement-corrected saturation intensity  $I_{sat}^{enh} = 0.3 \cdot I_{sat}^{SC} \approx 4.4 \text{ kW/cm}^2$ .

In the last part of the paper, we discuss the possible onset of bistability effects in this system. Bistability is the situation when two possible outputs correspond to a single input. In our case the input is the *incident beam*, while the output is the *reflected beam*. Bistability manifests itself as an hysteresis cycle when plotting the input-*vs*-output characteristic of the system.

We follow the elegant method developed for excitonic polaritons in Ref. [5], and deduce the main experimentally observable quantity, the reflected beam intensity, from the population of the excited state using the TCMT equations. The emergence of bistability in ISB systems has been previously theoretically approached in Ref. [15] (charge-transfer-induced optical bistability) and Ref. [14]

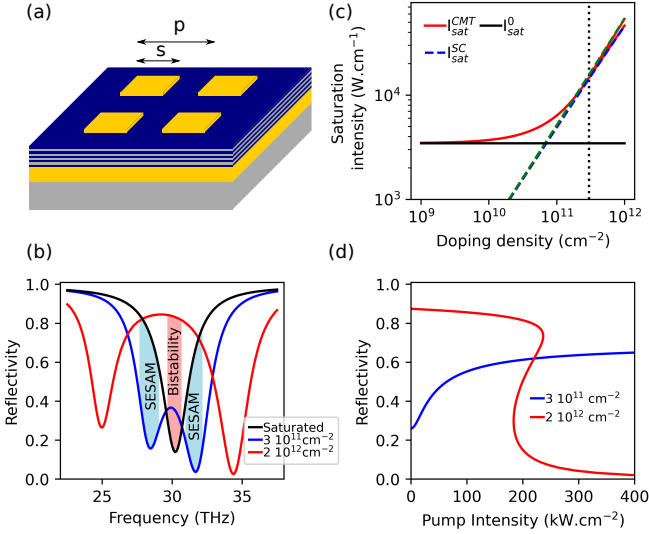


Figure 3. (a) Schematics of the patch-cavity configuration to be employed.  $s$  is the patch size, and  $p$  is the period. (b) FEM simulations of the reflectivity of the system for two different doping densities. Blue and red curves: low incident power, the polaritonic states are present. Black curve: high incident power, only the cavity resonance is visible. The structure is an array of patch cavities, with period  $p = 2.2 \mu\text{m}$  and size  $s = 1.2 \mu\text{m}$ . (c) Saturation intensity of the coupled ISB-patch system in (a) as a function of  $n_s$ . The target doping is indicated in black dotted line. (d) Reflectivity of the two design samples, SESAM (blue,  $n_s = 3 \cdot 10^{11} \text{ cm}^{-2}$ ) and bistable (red,  $n_s = 2 \cdot 10^{12} \text{ cm}^{-2}$ ) as a function of pump intensity. (c) and (d) are obtained from TCMT. Note that in (d) we plot the reflectivity, which includes the cavity losses. The saturation condition  $\mathcal{A}^{ISB}/2$  is thus different from a twofold increase in reflectivity.

(absorption bistability). It is best demonstrated by expressing the intensity-dependent excited state population as a function of the coupled system's characteristics, assuming (without loss of generality) that the pump frequency is set to  $\omega = \omega_0$ :

$$I(n_2) = \frac{n_2 \hbar \omega_0 N_{qw} [2an_2 - (\gamma_{isb}(\gamma_{nr} + \Gamma_r) - an_s)]^2}{4\tau_{12}\gamma_{isb}\Gamma_r a(n_s - 2n_2)} \quad (17)$$

The derivation and its extension to the detuned pump ( $\omega \neq \omega_0$ ) are presented in Supplementary Material. From this expression, one can derive the minimal doping necessary to observe bistability as a function of the system's damping rates:

$$n_s > \frac{32\varepsilon\varepsilon_0 m^* L_{qw} \gamma_{isb} (\gamma_{nr} + \Gamma_r)}{f_w e^2} \quad (18)$$

For our sample and cavity architecture, this critical value is around  $n_s \geq 1.1 \cdot 10^{12} \text{ cm}^{-2}$ . In order to illustrate the two different regimes proposed in Fig. 3(b) (SESAM and Bistability), we compare in Fig. 3(d) the reflected beam intensity in two experimental configurations: a saturable absorber sample with a doping level  $n_s = 3 \cdot 10^{11} \text{ cm}^{-2}$  pumped at the lower polariton frequency (blue), and a bistable sample with a doping level  $n_s = 2 \cdot 10^{12} \text{ cm}^{-2}$  pumped at the uncoupled ISB and cavity frequency  $\omega_0$  (red). We clearly evidence here a saturable absorber behaviour in the case of pumping at the polariton frequency (blue curve), and a bistable behaviour for pump intensities around  $100 \text{ kW/cm}^2$  (red curve). Reminding the definition of plasma frequency, Eq. 18 can be re-cast in the following form:

$$\frac{\Omega_{Rabi}}{\omega_{isb}} \cdot \frac{\Omega_{Rabi}}{\omega_{cav}} > \frac{2}{Q_{isb} Q_{cav}^{tot}} \quad (19)$$

While Eq. 19 does not add information with respect to Eq.18, it explicitly spells out the physical parameters governing bistability in an ISB polariton system, which has not been experimentally reported yet. In particular it shows the richness of engineering possibilities for ISB saturation in strong coupling with respect to the weak coupling case, nicely discussed in Ref. [32] and initially explored experimentally (but not observed) in Ref. [33].

In conclusion, we have demonstrated that the nature of absorption saturation for an ISB system changes radically when the system transitions from the weak to the strong light-matter coupling regime. In particular, in the SC regime the saturation intensity becomes doping dependent. This brings a new degree of freedom into the picture: we have provided design rules to engineer mid-IR systems with record-low saturation thresholds, and also to implement optically bistable devices. In particular the former result enables the development of SESAM mirrors operating in the mid-IR with low saturation intensities, a missing element from the current toolbox of mid-IR opto-electronics.

We thank I. Carusotto for thorough reading of the manuscript, and F.H. Julien, J-M. Manceau, L. Andreani, M. Helm, A. Bousseksou, S. Pirodda, for fruitful discussions. We acknowledge financial support from the European Union FET-Open Grant MIRBOSE (737017) and from the French National Research Agency (project TERASEL, ANR 18-CE24-0013 and project SOLID, ANR....).

- 
- [1] R. W. Boyd, *Nonlinear Optics*. Amsterdam: Elsevier, 3 ed., 2008.  
 [2] U. Keller, D. A. B. Miller, G. D. Boyd, T. H. Chiu, J. F.

Ferguson, and M. T. Asom, "Solid-state low-loss intracavity saturable absorber for nd:y:lf lasers: an antiresonant semiconductor fabry-perot saturable absorber,"

- Opt. Lett.*, vol. 17, pp. 505–507, Apr 1992.
- [3] B. Willenberg, J. Maurer, B. W. Mayer, and U. Keller, “Sub-cycle time resolution of multi-photon momentum transfer in strong-field ionization,” *Nature Communications*, vol. 10, pp. 1–8, dec 2019.
- [4] A. Tredicucci, Y. Chen, V. Pellegrini, M. Börger, and F. Bassani, “Optical bistability of semiconductor microcavities in the strong-coupling regime,” *Phys. Rev. A*, vol. 54, pp. 3493–3498, Oct 1996.
- [5] A. Baas, J. P. Karr, H. Eleuch, and E. Giacobino, “Optical bistability in semiconductor microcavities,” *Phys. Rev. A*, vol. 69, p. 023809, Feb 2004.
- [6] M. Helm, “The basic physics of intersubband transitions,” in *Semiconductors and Semimetals* (H. Liu and F. Capasso, eds.), vol. 62, ch. 1, pp. 1–99, Elsevier, 1999.
- [7] J. Faist, F. Capasso, D. L. Sivco, C. Sirtori, A. L. Hutchinson, and A. Y. Cho, “Quantum cascade laser,” *Science*, vol. 264, no. 5158, pp. 553–556, 1994.
- [8] A. Baranov and E. Tournie, *Semiconductor lasers : fundamentals and applications*. Woodhead Publishing, 2013.
- [9] E. Rosencher, B. Vinter, P. Piva, and K. (Firm), *Optoelectronics*. Knovel Library, Cambridge University Press, 2002.
- [10] We left out an angular factor that is of the order of unity for a vast range of incidence angles.
- [11] F. H. Julien, J. Lourtioz, N. Herschkorn, D. Delacourt, J. P. Pocholle, M. Papuchon, R. Planel, and G. Le Roux, “Optical saturation of intersubband absorption in GaAs-Al<sub>x</sub>Ga<sub>1-x</sub>As quantum wells,” *Applied Physics Letters*, vol. 53, no. 2, pp. 116–118, 1988.
- [12] K. L. Vodopyanov, V. Chazapis, C. C. Phillips, B. Sung, and J. S. Harris, “Intersubband absorption saturation study of narrow III-V multiple quantum wells in the  $\lambda = 2.8\text{-}9\ \mu\text{m}$  spectral range,” *Semiconductor Science and Technology*, vol. 12, pp. 708–714, jun 1997.
- [13] J. Y. Duboz, E. Costard, E. Rosencher, P. Bois, J. Nagle, J. M. Berset, D. Jaroszynski, and J. M. Ortega, “Electron relaxation time measurements in gaas/algaas quantum wells: Intersubband absorption saturation by a free electron laser,” *Journal of Applied Physics*, vol. 77, no. 12, pp. 6492–6495, 1995.
- [14] S. Zanotto, F. Bianco, L. Sorba, G. Biasiol, and A. Tredicucci, “Saturation and bistability of defect-mode intersubband polaritons,” *Phys. Rev. B*, vol. 91, p. 085308, Feb 2015.
- [15] M. Seto and M. Helm, “Charge transfer induced optical bistability in an asymmetric QW structure,” *Applied Physics Letters*, vol. 60, no. 7, pp. 859–861, 1992.
- [16] M. ZaÅ, uÅ¼ny and C. Nalewajko, “Coupling of infrared radiation to intersubband transitions in multiple quantum wells: The effective-medium approach,” *Phys. Rev. B*, vol. 59, pp. 13043–13053, May 1999.
- [17] In thin slabs the absorption is actually governed by the quantity  $\Im(1/\varepsilon_{zz})$ , which in this case can be straightforwardly re-written as  $\frac{1}{\varepsilon_{zz}} = \frac{1}{\varepsilon_{avg}} \frac{(\omega^2 - \omega_{12}^2 + \omega_p^2)(\omega^2 - \omega_{12}^2) + \gamma^2 \omega^2 - i\gamma\omega\omega_p^2}{(\omega^2 - \omega_{12}^2)^2 + \gamma^2 \omega^2}$  proving the linear dependence between the plasma frequency and ISB absorption.
- [18] M. Jeannin, T. Bonazzi, D. Gacemi, A. Vasanelli, L. Li, A. G. Davies, E. Linfield, C. Sirtori, and Y. Todorov, “Absorption engineering in an ultrasubwavelength quantum system,” *Nano Letters*, vol. 20, no. 6, pp. 4430–4436, 2020. PMID: 32407632.
- [19] The mathematics behind this effect is reminiscent of the one behind the gain clamping phenomenon in lasers.
- [20] S. Pirotta, N.-L. Tran, G. Biasiol, A. Jollivet, P. Crozat, J.-M. Manceau, A. Bousseksou, and R. Colombelli, “Ultra-fast amplitude modulation of mid-ir free-space beams at room-temperature,” *arXiv*, p. 2006.12215, 2020.
- [21] I. Roland, A. Borne, M. Ravarolo, R. D. Oliveira, S. Suffit, P. Filloux, A. Lemaitre, I. Favero, and G. Leo, “Frequency doubling and parametric fluorescence in a four-port aluminum gallium arsenide photonic chip,” *Opt. Lett.*, vol. 45, pp. 2878–2881, May 2020.
- [22]  $\gamma_i$  is the inverse of a time. It is defined as  $\gamma_i = \omega_i/Q_i$ , with  $Q_i$  a quality factor.
- [23] F. Alpegiani and L. C. Andreani, “Semiclassical theory of multisubband plasmons: Nonlocal electrodynamics and radiative effects,” *Physical Review B*, vol. 90, p. 115311, Sept. 2014.
- [24] C. A. Balanis, *Antenna Theory: Analysis and Design*. USA: Wiley-Interscience, 2005.
- [25] Y. Todorov, A. M. Andrews, R. Colombelli, S. De Liberato, C. Ciuti, P. Klang, G. Strasser, and C. Sirtori, “Ultrastrong light-matter coupling regime with polariton dots,” *Physical Review Letters*, vol. 105, p. 196402, 2010.
- [26] J. Lee, N. Nookala, J. S. Gomez-Diaz, M. Tymchenko, F. Demmerle, G. Boehm, M.-C. Amann, A. AlÅ<sup>1</sup>, and M. A. Belkin, “Ultrathin second-harmonic metasurfaces with record-high nonlinear optical response,” *Advanced Optical Materials*, vol. 4, no. 5, pp. 664–670, 2016.
- [27] M. Hakl, Q. Y. Lin, S. Lepillet, M. Billet, J.-F. Lampin, S. Pirotta, R. Colombelli, W. J. Wan, J. C. Cao, H. Li, E. Peytavit, and S. Barbieri, “Ultra-fast quantum-well infrared photodetectors operating at 10  $\mu\text{m}$  with flat response up to 70 ghz at room temperature,” *arXiv 2007.00299*, 2020.
- [28] The value of the radiative damping accounts for the fact that cavities are arranged in an array with subwavelength spacing, and is thus larger than in the case of an isolated cavity.
- [29] C. Bohren and D. Huffman, *Absorption and Scattering of Light by Small Particles*. Wiley Science Series, Wiley, 2008.
- [30] T. J. Seok, A. Jamshidi, M. Kim, S. Dhuey, A. Lakhani, H. Choo, P. J. Schuck, S. Cabrini, A. M. Schwartzberg, J. Bokor, E. Yablonovitch, and M. C. Wu, “Radiation engineering of optical antennas for maximum field enhancement,” *Nano Letters*, vol. 11, no. 7, pp. 2606–2610, 2011. PMID: 21648393.
- [31] C. Feuillet-Palma, Y. Todorov, A. Vasanelli, and C. Sirtori, “Strong near field enhancement in THz nano-antenna arrays,” *Scientific reports*, vol. 3, p. 1361, 03 2013.
- [32] M. Zaluzny, “Saturation of intersubband absorption and optical rectification in asymmetric quantum wells,” *Journal of Applied Physics*, vol. 74, no. 7, pp. 4716–4722, 1993.
- [33] K. Craig, B. Galdrikian, J. N. Heyman, A. G. Markelz, J. B. Williams, M. S. Sherwin, K. Campman, P. F. Hopkins, and A. C. Gossard, “Undressing a collective intersubband excitation in a quantum well,” *Phys. Rev. Lett.*, vol. 76, pp. 2382–2385, Mar 1996.